Temperature dependence of microstructure in Zn-Al alloys

Popović, Stanko; Gržeta, Biserka; Hanžek, Branko; Hajster, Snježana

Source / Izvornik: **Fizika A, 1999, 8, 173 - 182**

Journal article, Published version
Rad u časopisu, Objavljena verzija rada (izdavačev PDF)

Permanent link / Trajna poveznica: https://urn.nsk.hr/urn:nbn:hr:217:974557

ISSN 1330–0008
CODEN FIZAE4

TEMPERATURE DEPENDENCE OF MICROSTRUCTURE IN Zn-Al ALLOYS

STANKO POPOVIĆ[a], BISERKA GRŽETA[b], BRANKO HANŽEK[c]
and SNJEŽANA HAJSTER[a]

[a] *Physics Department, Faculty of Science, University of Zagreb, Bijenička cesta 32, 10001 Zagreb, Croatia*

[b] *"R. Bošković" Institute, Bijenička cesta 54, 10001 Zagreb, P.O.Box 1016, Croatia*

[c] *Ministry of Education, Trg burze 6, 10000 Zagreb, Croatia*

Dedicated to Professor Boran Leontić on the occasion of his 70$^{\mathbf{th}}$ birthday

Received 10 December 1999; Accepted 28 February 2000

The temperature dependence of microstructure in Zn-Al alloys, transferred to the equilibrium state by quenching from the solid solution temperature, T_{SS}, to room temperature (RT) and prolonged ageing at RT, was studied *in situ* by X-ray powder diffraction. Instead of the phase transitions expected according to the phase diagram, namely $\alpha(\mathrm{M}/\beta) + \beta \rightarrow \alpha' + \alpha(\mathrm{M}/\alpha') \rightarrow \alpha_{\mathrm{SS}}$ for the alloy with 54 at% Zn and $\alpha(\mathrm{M}/\beta) + \beta \rightarrow \alpha' + \beta \rightarrow \alpha_{\mathrm{SS}}$ for the alloy with 62 at% Zn, the following sequence was observed for both alloys: $\alpha(\mathrm{M}/\beta) + \beta \rightarrow \alpha' + \beta + \alpha(\mathrm{M}/\alpha', \beta) \rightarrow \alpha' + \beta \rightarrow \alpha_{\mathrm{SS}}$. In the cooling run, a temperature hysteresis in reversal phase transitions was observed. During a repeated heating, the microstructure depended on the previous thermal treatment of the alloys.

PACS numbers: 61.50.-f, 64.70, 64.75.-p, 64.75.+g, 65.70.+y UDC 548.73

Keywords: Zn-Al alloys, solid solution, phase transition, phase diagram, X-ray powder diffraction

1. *Introduction*

Physical and chemical properties, microstructure and phase diagram of the system Al-Zn have been studied by many authors. Most of the collected knowledge can be found in a recent comprehensive monograph edited by H. Löffler [1], containing about 700 references. Zinc atoms do not form intermetallic phases with

aluminium atoms. The atomic radius of Al atom is 0.143 nm, while the one of Zn atom is about 0.134 nm. This difference has a great influence on the microstructure of Al-Zn alloys.

The solid solubility of Zn in Al is 0.85 at%, while the one of Al in Zn is less than 0.5 at% at room temperature (RT, 298 K). The solubility of Zn in Al increases with temperature and reaches $\approx$ 67 at% at about 655 K [1]. The Al-Zn alloys rapidly quenched from the solid-solution temperature, T_{SS} (*e.g.* $T_{\mathrm{SS}} = 625$ K for the alloy with the initial Zn content, x_{Zn}, of 39.5 at% [1]) to RT are supersaturated. They decompose to a two-phase system (at least up to $x_{\mathrm{Zn}} = 44$ at% [2,3]), consisting of the fcc α(M/GPZ)-phase (M, the matrix) in a metastable equilibrium with a dense system of Guinier-Preston zones (GPZ), having about 70 at% Zn. On ageing, at RT or at elevated temperature, the decomposition of the quenched alloys proceeds in a number of phase transitions. The longest decomposition sequence is the following: spherical GPZ (fcc, fully coherent with M, having the radius of 1 to 2 nm) $\rightarrow$ ellipsoidal GPZ (fcc, fully coherent with M) $\rightarrow$ rhombohedrally distorted α'_{R}-phase (partially coherent with M, having the mean particle radius of the order of 10 nm) $\rightarrow$ metastable α'-phase (fcc, partially coherent with M) $\rightarrow$ β(Zn)-phase (hexagonal, incoherent with M) [1–3]. The number of intermediate metastable phases during the decomposition is reduced with the decrease of the ageing temperature. For ageing at RT, a direct transition of the big GPZ to β(Zn) precipitates is possible [1,3]. The decomposition process is mainly governed by the quenched-in vacancies. The binding energy of the vacancy-solute atom pair is estimated as 0.13(3) eV at RT [1].

After a prolonged ageing, *i.e.* after the completion of the decomposition process, the fcc α(M/β)-phase (having $\approx$ 99 at% Al) is in a stable equilibrium with β(Zn) precipitates which may be of a micrometer size (having $\approx$ 99.5 at% Zn). The ageing time necessary to reach the equilibrium state decreases with the increase of x_{Zn} and the ageing temperature. The latter strongly influences the diffusion rate of Zn atoms inside the matrix crystal lattice [1–3].

On the basis of a number of papers, most of them being referred to in Ref. [1], the phase diagram of the system Al-Zn has been established and accepted in the literature [1,4].

In spite of a very extensive literature on the Al-Zn system, a more detailed and accurate investigation of the dependence of microstructure on the composition, temperature and thermal treatment of the alloys has been undertaken recently [2,3,5–9]. Therefore, the Al-Zn alloys, having undergone different thermal treatments, were studied in detail by means of X-ray powder diffraction (XRD). The alloys of different composition, quenched rapidly from T_{SS} to RT, were subjected to ageing at RT or at elevated temperature, and the precipitation processes in supersaturated solid solutions were followed. Also, the alloys of different composition, having reached the equilibrium state, were subjected to the gradual change of temperature, from RT to T_{SS} and back to RT, and their microstructure was followed *in situ* by XRD. These studies have provided much new information, *e.g.* about the zinc content in M, for different types of precipitates, P, in contact with it, and the effect of strains occuring at the M/P interface on the unit-cell parameters of M, $a[\alpha(\mathrm{M/P})]$, of the

intermediate phase α', $a(\alpha')$, and of the solid solution α_{SS}, $a(\alpha_{SS})$. Thirteen Al-Zn alloys, with x_{Zn} varying from 4.5 to 62 at%, were studied in detail by XRD. Partial results on the alloys in the Zn-rich region, having $x_{Zn} = 54$ at% and $x_{Zn} = 62$ at%, have been given in Refs. [8,9], while a more detailed description on the temperature behaviour of microstructure in these alloys is given in the present paper.

2. Experimental

A detailed procedure of the preparation of alloys is given in Refs. [2,3,7]. The powder samples for XRD were prepared by filing the bulk alloys, produced from components of purity 4N. The samples were annealed in a vertical furnace, in the region of the solid solution temperature (up to 770 K) for 1 hour and quenched inside the furnace in water at RT. A vertical tube, long one meter and full of water, was inserted into the furnace just before the quench. The free-fall path of the sample to the water surface was about 10 mm; after that the sample continued to fall through the water column inside the tube. The powders were wrapped in a thin Al-foil having the thickness of 0.05 mm, perforated with hundreds of small holes, made by a needle, in order to increase the quenching rate, which was estimated to 10^5 K/s. The as-quenched alloys, being in a supersaturated state, were subjected to a prolonged ageing at RT. Having reached the equilibrium state [2,3], the alloys were heated from RT to T_{SS} and then cooled to RT, at a rate of about 2K per minute, inside the high-temperature attachment of a Philips diffractometer. The heating/cooling of the alloys was stopped at a series of temperatures (for 15 to 20 min) in order to scan the prominent diffraction line profiles. Two heating and cooling cycles, between RT and T_{SS}, were performed with the same specimen, for both Zn-rich alloys, with 54 and 62 at% Zn. The samples were exposed either to air (10^5 Pa) or to a low air pressure (10^{-3} Pa), but no effect of oxidation was observed by XRD. Several experiments were performed with each alloy and reproducible results were obtained.

In the derivation of unit-cell parameters of the phases α, α', α_{SS} and β(Zn) all precautions were undertaken in order to minimize the systematic aberrations influencing diffraction line positions [10]. The derivation of the unit-cell parameters was based on the measurement of the angular separation between (neighbouring) diffraction lines rather than on the measurement of angular positions of diffraction lines, following the refinement of experimental data described in Ref. [11].

3. Results and discussion

Instead of the phase transitions expected according to the phase diagram, namely $\alpha(M/\beta)+\beta(Zn) \rightarrow \alpha'+\alpha(M/\alpha') \rightarrow \alpha_{SS}$ for the alloy with 54 at% Zn, and $\alpha(M/\beta)+\beta(Zn) \rightarrow \alpha'+\beta \rightarrow \alpha_{SS}$ for the alloy with 62 at% Zn, the following sequence has been observed for both alloys:

$$\alpha(M/\beta)+\beta(Zn) \rightarrow \alpha'+\beta(Zn)+\alpha(M/\alpha',\beta) \rightarrow \alpha'+\beta(Zn) \rightarrow \alpha_{SS}.$$

This indicates that a correction in the phase diagram of the system Al-Zn is necessary.

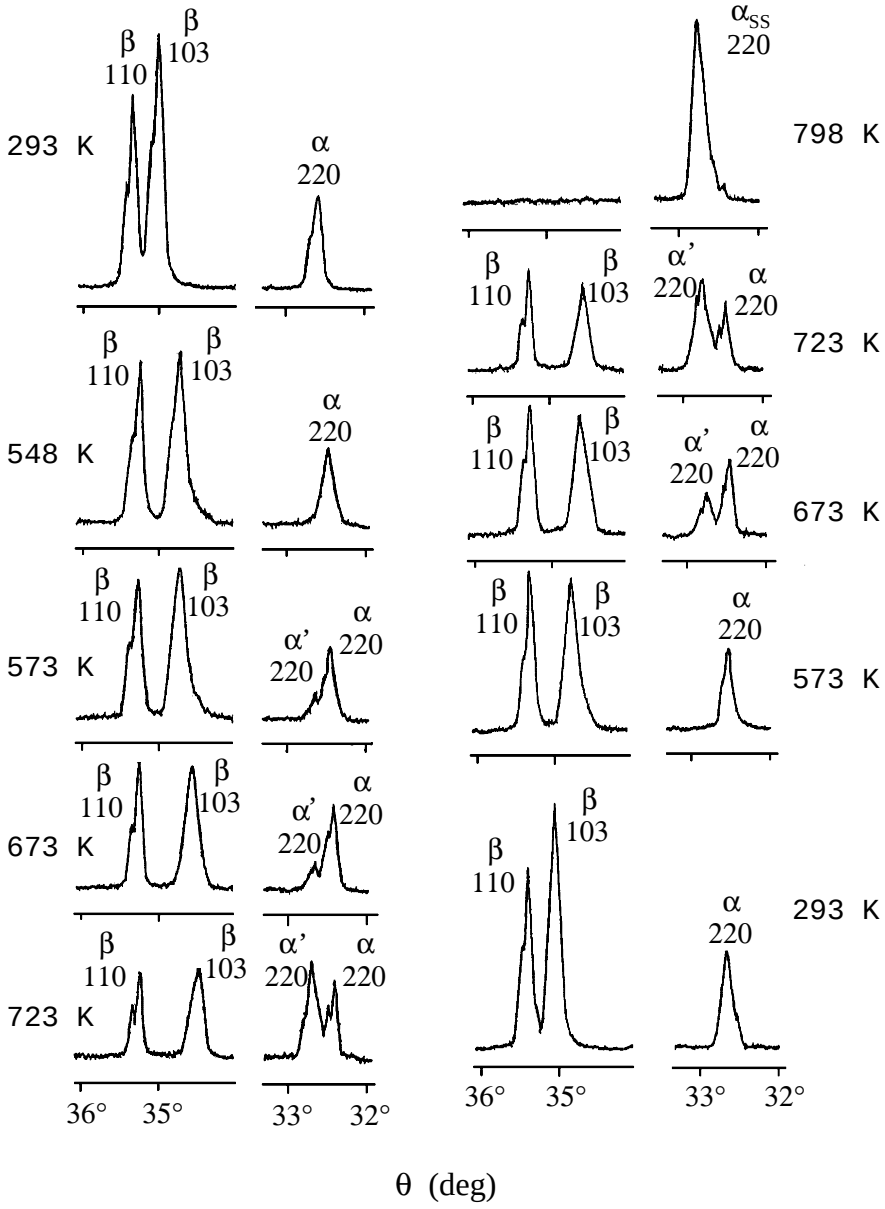

Fig. 1. Prominent diffraction lines of the alloy Al-*54 at%* Zn *at different temperatures, including both (the second) heating and cooling cycle. Radiation: monochromatized (graphite)* Cu$K\alpha$*, counter: proportional.*

Prominent diffraction lines, at medium Bragg angles, of the alloy with 54 at% Zn, scanned *in situ* at different temperatures, including a complete heating and cooling cycle, are shown in Fig. 1. In fact, Fig. 1 shows the second heating and cooling cycle of the alloy. The dependence of the unit-cell parameter, a, of the phases α, α' and α_{SS} in the alloy Al-54 at% Zn on temperature during the first heating and cooling cycle is shown in Fig. 2a. The same dependence during the second heating and cooling cycle, for the same specimen, is shown in Fig. 2b.

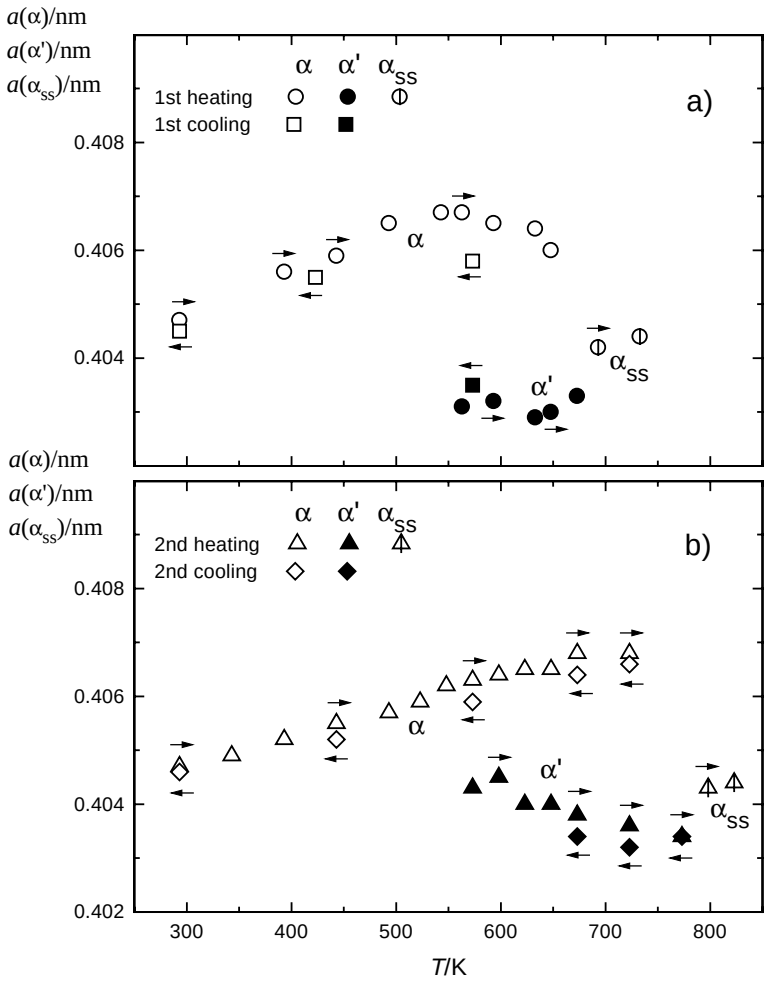

Fig. 2. The dependence of the unit-cell parameter, a, of the phases α, α' and α_{SS} in the alloy Al-*54 at%* Zn, *for the same specimen, on temperature* a*) during the first heating from* RT *to* T_{SS} *and cooling to* RT *and* b*) during the second heating from* RT *to* T_{SS} *and cooling to* RT. *The arrows indicate the sense of temperature change. The size of shown marks is approximately equal to estimated standard deviation (e.s.d.) in* a.

Figure 3 shows the temperature dependence of the spacing d_{103} of the phase β(Zn) in the alloy Al-54 at% Zn during the first (1) and second (2) heating and cooling cycles of the same specimen. The comparison of the temperature dependence of the unit-cell parameters a and c of the phase β(Zn) in the alloy Al-54 at% Zn during the first (1) and second (2) heating of the same specimen is shown in Figs. 4 and

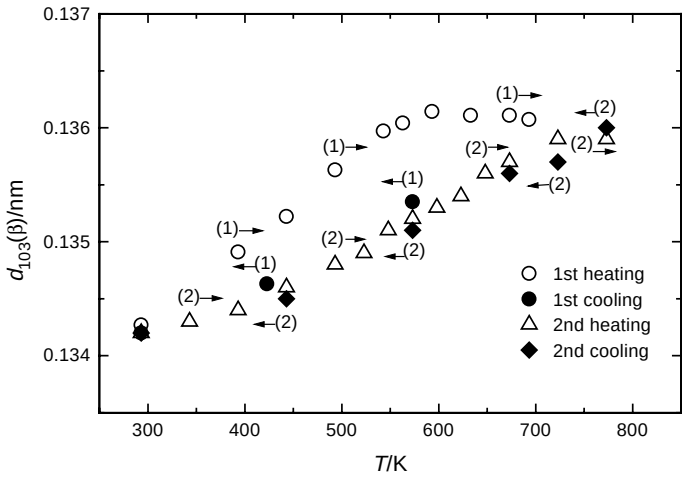

Fig. 3. The dependence of the spacing d_{103} of the phase β(Zn) in the alloy Al-*54 at%* Zn, *for the same specimen, on temperature (1) during the first heating and cooling and (2) during the second heating and cooling. The arrows indicate the sense of temperature change. The shown marks are larger than the e.s.d. in d_{103}.*

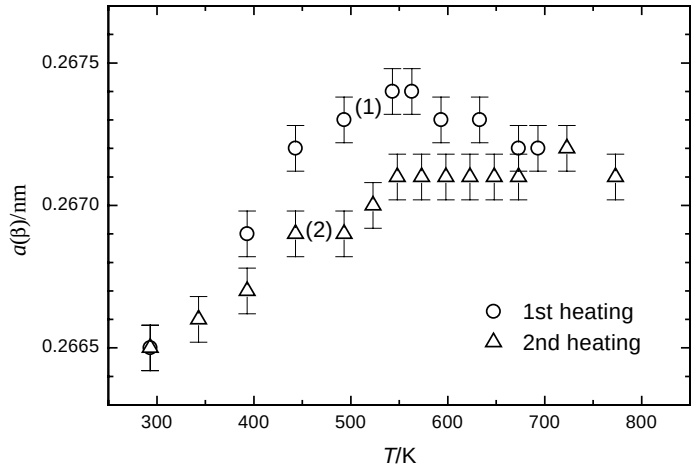

Fig. 4. The comparison of the dependence of the unit-cell parameter $a(\beta)$ of the phase β(Zn) in the alloy Al-*54 at%* Zn, *for the same specimen, on temperature during (1) the first and (2) the second heating from* RT *to T_{SS}. The points corresponding to the cooling runs are not shown. Vertical bars indicate* e.s.d. *in $a(\beta)$.*

5, respectively. Similar temperature behaviour has been also observed for the alloy Al-62 at% Zn.

One can see from Figs. 2 to 5 that the temperature dependence of the microstructure during the first heating/cooling cycle is different from that during the second heating/cooling cycle; this point will be discussed later in more detail.

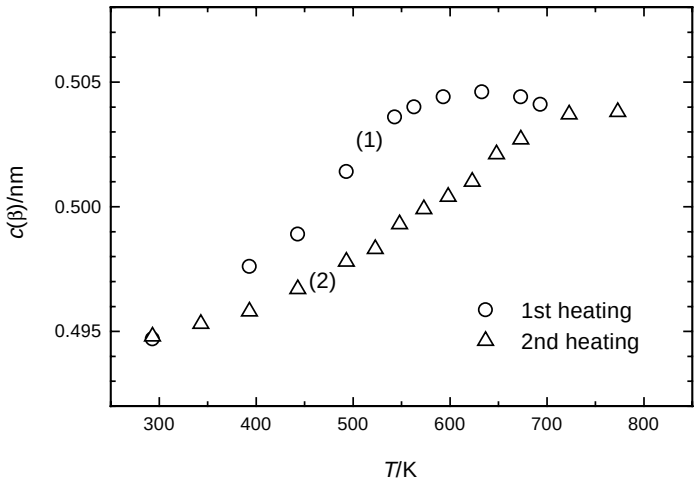

Fig. 5. The comparison of the dependence of the unit-cell parameter $c(\beta)$ of the phase β(Zn) in the alloy Al-*54 at%* Zn*, for the same specimen, on temperature (1) during the first and (2) second heating from* RT *to* T_{SS}*. The points corresponding to the cooling runs are not shown. The size of the shown marks are approximately equal to e.s.d. in* $c(\beta)$*.*

It has been shown in previous papers [2,3,8] that the unit-cell parameter of the $\alpha(\mathrm{M}/\beta)$-phase, in equilibrium with the β(Zn)-phase reached after quenching and prolonged ageing, does not depend on the initial alloy composition, amounting 0.40469(6) nm at RT. For comparison, the unit-cell parameter of pure Al at RT is 0.40494(3) nm. The unit-cell parameters of the β(Zn)-phase, in equilibrium with the $\alpha(\mathrm{M}/\beta)$-phase, are close to the ones of pure Zn at RT, $a = 0.2665(2), c = 0.4947(3)$ nm (space group $P6_3/mmc$). However, for the alloys, which reach the equilibrium state by slow cooling from T_{SS} to RT, the unit-cell parameter of the $\alpha(\mathrm{M}/\beta)$-phase is 0.40445(10) nm at RT, regardless of the initial alloy composition [2,3,8]. The difference between these two equilibrium values of $a[\alpha(\mathrm{M}/\beta)]$ may be explained by different contents of Zn retained in the matrix, as a consequence of different thermal treatments.

As the temperature of the alloy increases, a decrease of the diffraction line intensities of both $\alpha(\mathrm{M}/\beta)$- and β(Zn)-phases takes place, due to increased thermal vibration amplitudes of the atoms. Also, a gradual shift of diffraction lines toward smaller Bragg angles, caused by thermal expansion, is observed (Fig. 1). The phase β(Zn) exhibits an anisotropy in thermal expansion (which can be followed, for instance, from the temperature dependence of the separation of its diffraction lines

110 and 103 in Fig. 1). This is several times larger along the c-axis than along the a-axis (Table 1). Besides, a change of the shape of the β(Zn) precipitates on heating is observed, from the broadening of diffraction lines with $l \neq 0$, *e.g.* 002 and 103, in relation to the diffraction lines 100 and 110 (Fig. 1). The dimension of the β(Zn) precipitates along the c-axis decreases as the temperature increases; the Zn atoms, leaving β(Zn) precipitates, are dominantly those which form lattice planes (001). The concentration of vacancies in the β(Zn)-phase increases with temperature, this affecting the temperature dependence of its unit-cell parameters (Figs. 3, 4 and 5).

TABLE 1. The average thermal expansion coefficient, α_T, of the phases α(M/β) and β(Zn) in the temperature interval from RT *to 490* K *determined for the first (1) and second (2) heating of the same specimen of the alloy with 54 at%* Zn *and of the alloy with 62 at%* Zn.

Alloy	$\alpha_T \times 10^5$ K	Phase		
		α(M/β)	β(Zn)	
			along a-axis	along c-axis
$x_{Zn} = 54$ at%	(1)	2.2(3)	1.5(2)	6.8(5)
	(2)	1.2(2)	0.8(1)	3.1(3)
$x_{Zn} = 62$ at%	(1)	2.4(3)	1.2(2)	7.0(5)
	(2)	1.7(3)	1.0(2)	4.0(4)

The unit-cell parameter, a, of the α(M/β)-phase changes linearly up to about 490 K during the first heating (Fig. 2a). At higher temperatures, a pronounced partial dissolution of the β(Zn)-phase in the α(M/β)-phase takes place; this effect compensates or even reverses the change of a[α(M/β)] with temperature (Fig. 2a). Above about 550 K, a partial transition of the β(Zn)-phase, and probably a partial transition of the α(M/β)-phase, into the fcc α'-phase takes place (Figs. 2a and b). The unit-cell parameter a of the α'-phase is about 0.9% smaller than that of the α(M/α',β)-phase at 560 K during the first heating, due to different contents of Zn in these phases. On further heating, the composition of the phases changes; the α(M/α',β)-phase disappears at about 650 K (during the first heating), the α'-phase remaining in coexistence with the β(Zn)-phase (Fig. 2a). The β(Zn)-phase finally disappears at about 700 K (during the first heating), and the fcc solid solution, α_{SS}, is formed (Figs. 3, 4 and 5). The unit-cell parameter of the solid solution, $a(\alpha_{SS})$, at 700 K is 0.4045(1) and 0.4038(1) nm for the alloys with 54 and 62 at% Zn, respectively (Figs. 2a and b).

During the first heating and cooling cycle, a temperature hysteresis in reversal phase transitions is observed (Figs. 2 and 3). In the repeated, second, heating of the same specimen, a temperature delay in phase transitions of several tens of K takes place in relation to the first heating (Figs. 3,4 and 5). During the second cooling, the microstructural parameters exhibit approximately the same

dependence on temperature as during the first cooling and the second heating of the alloy (Figs. 2b and 3).

The average value of the thermal expansion coefficients, α_{T}, of the phases $\alpha(\mathrm{M}/\beta)$ and $\beta(\mathrm{Zn})$ have been determined in the temperature interval from RT to 490 K. Above that temperature, a partial dissolution of the $\beta(\mathrm{Zn})$-phase in $\alpha(\mathrm{M}/\beta)$-phase takes place, causing a change in composition of the phase $\alpha(\mathrm{M}/\beta)$. One can notice an unusual change of $a(\alpha)$, $d_{103}(\beta)$, $a(\beta)$ and $c(\beta)$ with temperature above ≈ 550 K during the first heating (Figs. 2,3,4 and 5). Therefore, the physical meaning of α_{T}, which would be related to higher temperatures, is questionable. The average thermal expansion coefficient of the phases $\alpha(\mathrm{M}/\beta)$ and $\beta(\mathrm{Zn})$ in the interval from RT to 490 K, measured during the first (1) and second (2) heating of the alloy with 54 at% Zn and of the alloy with 62 at% Zn, is given in Table 1.

4. Conclusion

The dependence of unit-cell parameters on temperature during the first heating is different from the dependence during the first cooling and the second heating and cooling of one and the same specimen. This difference may be explained in terms of a different microstructure of the alloy existing before the first heating and before the second heating. The initial microstructure is formed after rapid quenching the alloy from a temperature above T_{SS} to RT and after a prolonged ageing at RT, this resulting in an equilibrium state $\alpha(\mathrm{M}/\beta)+\beta(\mathrm{Zn})$. One may suppose that the precipitates $\beta(\mathrm{Zn})$ are not uniformly distributed, and residual strains in the $\alpha(\mathrm{M}/\beta)$-phase around the $\beta(\mathrm{Zn})$ precipitates are present. The first heating of the sample is slow, with a rate of ≈ 2 K/min, and the sample is held for 15 to 20 min at a number of temperatures in order to record diffraction patterns. Therefore, one may suppose that the strains are annealed during the first heating. The first cooling is performed in a similar way. This results in a microstructure at RT which is different from the initial microstructure at RT, concerning the size and shape of the $\beta(\mathrm{Zn})$ precipitates, their distribution in the matrix, and strains in the $\alpha(\mathrm{M}/\beta)$-phase around the $\beta(\mathrm{Zn})$ precipitates. The strains are mostly annealed during the first slow heating and slow cooling of the alloy. A very important fact is that the number of vacancies at RT after the slow heating and cooling cycle may be much smaller than in the as-quenched alloy. This fact has a dominant influence on the diffusion rate of Zn atoms, explaining the delay in phase transitions during the second heating. Therefore, the present study shows that the previous thermal treatment has a dominant influence on the microstructure of the alloys.

The same sequence of the phase transitions observed in the studied alloys (having $x_{\mathrm{Zn}} = 54$ at% and $x_{\mathrm{Zn}} = 62$ at%) indicates that the eutectoid point at ≈ 550 K, shown in the phase diagram for the transition $\alpha+\beta \leftrightarrow \alpha+\alpha$', should be shifted from the point at 59 at% Zn to a point between 48 and 54 at% Zn [8,9].

References

1) H. Löffler, *Structure and Structure Development in Al-Zn Alloys*, Akademie Verlag, Berlin (1995);

2) S. Popović, H. Löffler, B. Gržeta, G. Wendrock and P. Czurratis, Phys. Stat. Sol. (a) **111** (1989) 417;

3) S. Popović, B. Gržeta, V. Ilakovac, R. Kroggel, G. Wendrock and H. Löffler, Phys. Stat. Sol. (a) **130** (1992) 273;

4) H. Löffler, G. Wendrock and O. Simmich, Phys. Stat. Sol. (a) **132** (1992) 339;

5) S. Popović, B. Gržeta, H. Lŏffler and G. Wendrock, Phys. Stat. Sol. (a) **140** (1993) 341;

6) S. Popović, B. Gržeta, H. Löffler and G. Wendrock, Fizika A **4** (1995) 529;

7) S. Popović, B. Gržeta, H. Löffler and G. Wendrock, *Lattice Constant of the Al-rich fcc α-Phase in Contact with Various Kinds of Precipitates*, in 1), pp. 212-241;

8) S. Popović and B. Gržeta, Croat. Chem. Acta **72** (1999) 621;

9) S. Popović and B. Gržeta, Mater. Sci. Forum **321-324** (2000) 635;

10) S. Popović, Crystal Res. Technol. **20** (1985) 552;

11) S. Popović, J. Appl. Cryst. **4** (1971) 240; **6** (1973) 122, 411.

OVISNOST MIKROSTRUKTURE SLITINA Zn-Al O TEMPERATURI

Primjenom rendgenske difrakcije istraživali smo temperaturnu ovisnost mikrostrukture slitina Zn-Al, koje su bile prevedene u ravnotežno stanje brzim kaljenjem s temperature čvrste otopine, T_{SS}, na sobnu temperaturu, te dugotrajnim starenjem pri sobnoj temperaturi. Umjesto faznih pretvorbi koje su se očekivale prema faznom dijagramu, naime $\alpha(\mathrm{M}/\beta) + \beta \rightarrow \alpha' + \alpha(\mathrm{M}/\alpha') \rightarrow \alpha_{\mathrm{SS}}$ za slitinu s 54 at% Zn, te $\alpha(\mathrm{M}/\beta) + \beta \rightarrow \alpha' + \beta \rightarrow \alpha_{\mathrm{SS}}$ za slitinu s 62 at% Zn, opazili smo sljedeći niz faznih pretvorbi za obje slitine: $\alpha(\mathrm{M}/\beta) + \beta \rightarrow \alpha' + \beta + \alpha(\mathrm{M}/\alpha', \beta) \rightarrow \alpha' + \beta \rightarrow \alpha_{\mathrm{SS}}$. Tijekom hlađenja slitina uočili smo temperaturnu histerezu za obrnute fazne pretvorbe. Tijekom ponovnog grijanja slitina od sobne temperature do T_{SS} utvrdili smo da mikrostruktura slitina ovisi o prethodnoj termičkoj obradi.